

# Low-Spin Ferric Porphyrin Complexes: Analysis of the Electronic Structure Based on Single-Crystal Electron Spin Resonance Measurements

Marianne P. Byrn, Bradley A. Katz, Nancy L. Keder, Keith R. Levan,  
Charles J. Magurany, Kathleen M. Miller, Jeffrey W. Pritt, and Charles E. Strouse\*

Contribution from the James D. McCullough X-ray Crystallography Laboratory, Department of Chemistry and Biochemistry, University of California, Los Angeles, California 90024.

Received September 27, 1982

**Abstract:** Single-crystal electron spin resonance  $g$  tensor determination for a low-spin ferric porphyrin complex can provide both an accurate description of spin distribution and a quantitative characterization of the axial ligand binding. Experimental  $g$  tensor determinations for a series of six low-spin (tetraphenylporphinato)iron(III) thiolate complexes illustrate the simple, but not intuitive, relationship between the orientation of the principal axes of the  $g$  tensor and the spin distribution. The axial thiolate ligands in this series of complexes cover a relatively wide range of  $\sigma$ -donor strength. Analysis of the crystal field parameters obtained from the principal  $g$  values reveals an excellent correlation between the tetragonality ( $\Delta$ ) and the  $pK_a$  of the corresponding thiol. On the other hand, the rhombicity ( $V/\Delta$ ) for this series of complexes is virtually independent of  $\sigma$ -donor strength of the axial ligand. This observation provides a basis for the prediction of spin density distribution in unsymmetrically ligated porphyrin complexes. Published single-crystal ESR data for several heme proteins are reevaluated in light of these results.

Experimental determination of the  $g$  tensor for a low-spin six-coordinate Fe(III) complex can provide a very detailed picture of the electronic structure. To a useful level of approximation, the wave functions and relative energies of the three iron  $d\pi$  orbitals are obtained. This information, in turn, provides a description of the spin distribution and a quantitative characterization of the metal-ligand binding. An important application of  $g$  tensor analysis has been the study of low-spin iron in the ferric form of heme proteins. Numerous investigators have discussed the extraction of crystal field parameters from the magnitudes of the principal  $g$  values.<sup>1-7</sup> Knowledge of the orientation of the principal axes of the  $g$  tensor with respect to the heme group and its associated axial ligands is, however, essential for a complete analysis. In the somewhat limited body of published single-crystal data from ferric heme proteins, it is found that the principal axis of the  $g$  tensor with the largest magnitude is within about 15° of the normal to the porphyrin plane, but efforts to rationalize the orientation of the two principal axes in the porphyrin plane have not been particularly successful. This results, in part, from a subtlety in the analysis of the "g tensor orientation" (i.e., the orientation of the principal axes of the  $g$  tensor) that has been overlooked by many investigators. The interpretation is also impeded by a lack of similar data for well-characterized "small-molecule" porphyrin complexes. The present report will point out an oversight in interpretation that has occurred repeatedly in the literature, describe and interpret the  $g$  tensor orientations for a series of low-spin (tetraphenylporphinato)iron(III) complexes, and reevaluate some of the published single-crystal ESR data for heme proteins.

In a 1957 analysis, Griffith<sup>1</sup> put forth a "very tentative" prediction that in the azide complex of metmyoglobin (Mb-azide) "the direction of the smallest  $g$  value lies along the orthogonal projection of the plane of the imidazole ring on the haem plane". In 1968 Helcké, Ingram, and Slade,<sup>8</sup> in another analysis of the same material, stated that "the minimum  $g$  value in the haem plane should be parallel to the projection of the histidine ring on that plane". These statements were based on the assumption that the

axial ligand (specifically the imidazole in Mb-azide) is responsible for the asymmetry of the  $g$  values in the heme plane. At this point the structure of myoglobin had been determined,<sup>9</sup> and it was indeed found that the minimum  $g$  value corresponded very closely to the projection of the coordinated imidazole on the heme plane. In 1969 Ingram<sup>10</sup> restated the interpretation in the following form: "...if the maximum  $g$  value...in the haem plane is associated with the  $y$  direction, the molecular orbital analysis implies that the  $d_{yz}$  orbit will be lying highest in the  $t_{2g}$  group, and therefore that the  $p$  orbital of the nitrogen of the histidine plane will be parallel to the  $y$  axis". In a more detailed and widely cited 1977 analysis, Taylor<sup>5</sup> stated that " $g_y$  indicates the direction in the heme plane associated with the greatest unpaired spin density"; i.e., "the two numerically largest  $g$  values define the plane and orientation of the orbital with the largest coefficient, the one most like the distribution of unpaired spin density in the complex".

All of these analyses are based, at least implicitly, on a model for the complex in which the projection of the plane of the axial ligand onto the heme plane contains two of the porphyrin nitrogen atoms; i.e., the principal axes of the rhombic component of the ligand field correspond to the cubic axes. In this case, as Taylor showed, the partially filled orbital lies in a plane defined by the two largest  $g$  values. However, it was recognized by Oosterhuis and Lang<sup>11</sup> (1969) that if from this configuration the rhombic component of the ligand field is rotated about the tetragonal axis,  $z$ , by the angle  $\theta$ , the principal axes of the  $g$  tensor rotate about  $z$  through the angle  $-\theta$ . Thus the plane defined by the partially filled orbital no longer corresponds, in general, to the principal axes of the  $g$  tensor. Unfortunately this observation, which was published in a paper on the Mössbauer effect in  $K_3Fe(CN)_6$ , seems to have been overlooked by most investigators of porphyrin complexes.

The implications of the analysis by Oosterhuis and Lang<sup>11</sup> are easily demonstrated. For a (porphinato)iron(III) complex with planar  $\pi$ -donating ligands in the axial coordination sites, two limiting cases correspond to two conformers with  $D_{2h}$  symmetry. These represent the situations where  $\theta = 0^\circ$  and  $\theta = 45^\circ$  (see Figure 1).

Conformer 1 in Figure 1 is the case treated explicitly by Taylor and others. An energy level diagram based on the hole model is given in Figure 2. This diagram shows the ground state and

(1) Griffith, J. S. *Nature (London)* **1957**, *180*, 30.

(2) Kotani, M. *Biopolymers Symp.* **1964**, *No. 1*, 65.

(3) Harris, G. *Theor. Chim. Acta* **1966**, *5*, 379.

(4) Weissbluth, M. "Hemoglobin, Cooperativity and Electronic Properties"; Springer-Verlag: Berlin, 1974.

(5) Taylor, C. P. S. *Biochim. Biophys. Acta* **1977**, *491*, 137.

(6) Bohan, T. L. *J. Magn. Reson.* **1977**, *26*, 109.

(7) Sato, M.; Ohya, T.; Morishima, I. *Mol. Phys.* **1981**, *42*, 475.

(8) Helcké, G. A.; Ingram, D. J. E.; Slade, E. F. *Proc. R. Soc. B* **1968**, *169*, 275.

(9) Stryer, L.; Kendrew, J. C.; Watson, H. C. *J. Mol. Biol.* **1964**, *8*, 96.

(10) Ingram, D. J. E. "Biological and Biochemical Applications of Electron Spin Resonance"; Plenum Press: New York, 1969; p 257.

(11) Oosterhuis, W. T.; Lang, G. *Phys. Rev.* **1969**, *178*, 439.

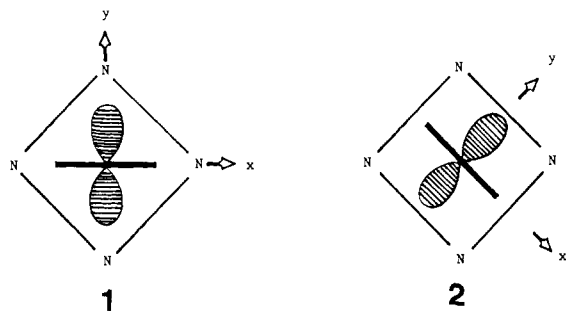


Figure 1. Two conformers of an idealized porphyrin complex. The plane of the axial ligand and orientation of the partially filled orbital  $d_{yz}$  are indicated.

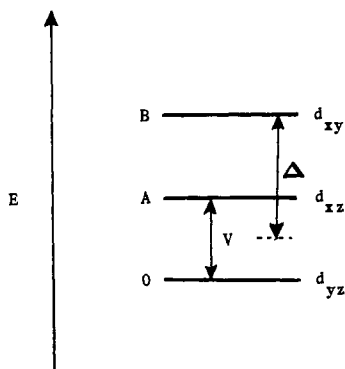


Figure 2. The energy level diagram for conformer 1.

the two low-lying excited states that can be mixed with the ground state by spin-orbit coupling. Definitions of the crystal field parameters  $V$  and  $\Delta$  are indicated.

The ground state corresponds to the hole (and the unpaired electron) occupying the  $d_{yz}$  orbital. In terms of one-electron energies the  $d_{yz}$  orbital is highest in energy by virtue of its interaction with filled  $\pi$  orbitals on both the porphyrin and the axial ligands.

First-order perturbation theory gives the following expression for the elements of the  $g$  tensor:<sup>12</sup>

$$|g_{ij}| = g_e + (2\lambda/A) \langle d_{yz} | L_i | d_{xz} \rangle \langle d_{xz} | L_j | d_{yz} \rangle + (2\lambda/B) \langle d_{yz} | L_i | d_{xy} \rangle \langle d_{xy} | L_j | d_{yz} \rangle$$

( $i, j = x, y, \text{ or } z$  and  $\lambda$  is the spin-orbit coupling constant). Expansion of the real  $d$  orbitals in terms of eigenfunctions of  $L_z$  and application of the appropriate angular momentum operators give the results

$$|g_{xx}| = g_e \quad |g_{yy}| = g_e + 2\lambda/B \quad |g_{zz}| = g_e + 2\lambda/A$$

These  $g$  values are in general accord with those obtained by Taylor from diagonalization of the energy matrix. While the treatment here represents a lower level of approximation than that used by Taylor, it reduces the argument to a simple symmetry analysis.

In the case of conformer 2 the three eigenfunctions of interest are described in the indicated (unconventional) coordinate system as  $d_{yz}$ ,  $d_{xz}$ , and  $d_{x^2-y^2}$ , where again the ground state corresponds to partial occupation of the  $d_{yz}$  orbital. Substitution of  $d_{xy}$  by  $d_{x^2-y^2}$  in the first-order expressions for the  $g$  values gives

$$|g_{xx}| = g_e + 2\lambda/B \quad |g_{yy}| = g_e \quad |g_{zz}| = g_e + 2\lambda/A$$

In contrast to the case of conformer 1, the plane of maximal spin density is now defined by the numerically largest and smallest  $g$  values.

Intermediate situations in which the lowest energy orbital is described as a linear combination of  $d_{xy}$  and  $d_{x^2-y^2}$  give rise to a nonzero value of  $g_{xy}$  but the same principal values.<sup>13</sup> Figure 3

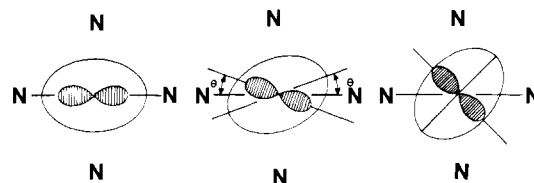


Figure 3. The relationship between the orientation of the partially filled orbital and the principal axes of the  $g$  tensor in the porphyrin plane.

shows the predicted behavior of the  $g$  tensor as the partially filled molecular orbital is rotated with respect to the porphyrin. The principal axes of the  $g$  tensor and the partially filled orbital are seen to rotate in opposite directions. Thus, in the porphyrin plane, the "direction of maximum spin density" is related to the direction of the largest in-plane  $g$  value by reflection through an Fe-N(pyrrole) vector.

The relationship between axial ligand orientation and  $g$  tensor orientation became evident in the course of experimental  $g$  tensor determinations for a series of six (tetraphenylporphyrinato)iron(III) complexes. These complexes were prepared as a part of an investigation of the solid-state equilibria exhibited by some sulfur-ligated ferric porphyrins. The structure and  $g$  tensor determination for the  $\text{Fe}^{\text{III}}\text{TPP}$  bis(benzenethiolate) anion have been reported previously.<sup>14</sup> The other five complexes are neutral species with the general formula  $\text{Fe}^{\text{III}}\text{P}(\text{SR})(\text{HSR})$  where R = phenyl (Ph), *m*-tolyl (*m*-Tol), benzyl (Bzl), or isoamyl (3-Me-1-Bu) and where P = tetraphenylporphyrinato (TPP) or the tetraphenylporphyrinato derivative in which one of the phenyl groups has been substituted in an ortho position with an amino group ( $\text{NH}_2\text{TPP}$ ).

## Experimental Section

**Structure Determinations.** All six complexes crystallize in triclinic lattices with one molecule per unit cell. The R = phenyl and P = TPP, R = phenyl and P =  $\text{NH}_2\text{TPP}$ , and R = *m*-tolyl and P = TPP complexes are isomorphous; these derivatives exist as a mixture of spin isomers. The structures of all of the thiol/thiolate complexes have been refined in the space group  $P\bar{1}$  which requires a disorder between the thiol and thiolate ligands. Detailed accounts of the syntheses and structure determinations will be published elsewhere.

**ESR Measurements.** All ESR measurements were made with an X-band spectrometer constructed from a variety of commercial components. The magnetic field was calibrated with an NMR gaussmeter, and the frequency was determined by use of a DPPH reference. Three crystals of each compound were used in the determination of the  $g$  tensor. These crystals were attached to quartz rods in approximately orthogonal orientations. An orientation matrix was determined for each crystal with a Syntex P1 automated diffractometer along with the  $\phi$  value of a flat face on the quartz rod. The sample was then transferred to an ESR spectrometer where  $g$  values were measured as a function of rotation about the rod axis. Angular measurements were recorded between the magnetic field direction and the flat face of the rod. The uncertainty in the angular measurements is approximately  $1^\circ$ , and the uncertainty in the measured  $g$  values is on the order of 0.002. A detailed description of the procedure by which the  $g$  tensor in the crystallographic coordinate system is extracted from the crystallographic and ESR measurements is published elsewhere.<sup>15</sup> All ESR data for the thiol/thiolate complexes were obtained at 77 K, except those for the R = phenyl and P = TPP derivative which were collected in the range 160–173 K. All X-ray measurements were carried out at 115 K, except those for the benzyl complex which were carried out at room temperature.

## Results and Discussion

**Analysis of the Principal  $g$  Values.** Principal  $g$  values obtained from the single-crystal measurements are summarized in Table I along with the derived<sup>5</sup> ligand field parameters. Also included in Table I are the average Fe-S distances for each structure. In this series of compounds there is an excellent correlation between the observed Fe-S distance and the axial component of the ligand

(13) Alternatively, one can choose a coordinate system fixed with respect to the porphyrin. In that case the in-plane orbital can be chosen as the  $d_{xy}$  orbital in both conformers, while the out-of-plane orbitals become linear combinations of  $d_{xz}$  and  $d_{yz}$ .

(14) Byrn, M. P.; Strouse, C. E. *J. Am. Chem. Soc.* **1981**, *103*, 2633.

(15) Byrn, M. P.; Strouse, C. E. *J. Magn. Reson.*, accepted for publication.

(12) Carrington, A.; McLachlan, A. D. "Introduction to Magnetic Resonance"; Harper and Row: New York, 1967.

Table I. Structural and Electronic Parameters for Sulfur-Ligated Ferric Porphyrin Complexes

	$g_1$	$g_2$	$g_3$	Fe-S <sup>a</sup>	pK <sub>a</sub>	$\Delta^f$	$V^f$	$V/\Delta^f$
(S-3-Me-1-Bu)(HS-3-Me-1-Bu)FeTPP	1.989	2.181	2.273	2.293 (2)	10.6 <sup>c</sup>	8.2	8.1	0.99
(SBzl)(HSBzl)FeTPP <sup>e</sup>	1.978	2.187	2.279	2.316 (1)	9.4 <sup>d</sup>	7.5	7.7	1.03
(SPh) <sub>2</sub> FeTPP <sup>1-g</sup>	1.962	2.215	2.336	2.336 (1)	6.5 <sup>d</sup>	6.5	6.4	0.98
(S- <i>m</i> -Tol)(HS- <i>m</i> -Tol)FeTPP	1.971	2.240	2.382	(2.45) <sup>b</sup>	6.6 <sup>d</sup>	6.3	5.9	0.93
(SPh)(HSPH)FeNH <sub>2</sub> TPP	1.965	2.242	2.368	2.32 (3) <sup>b</sup>	6.5 <sup>d</sup>	6.0	6.0	1.00
(SPh)(HSPH)FeTPP	1.966	2.244	2.364	2.339 (7) <sup>b</sup>	6.5 <sup>d</sup>	5.9	6.1	1.03

Direction Cosines of the Principal Axes of the $g$ Tensor in an Orthogonal Molecular Coordinate System <sup>h</sup>							
$g$	$x$	$y$	$z$	$g$	$x$	$y$	$z$
(S-3-Me-1-Bu)(HS-3-Me-1-Bu)FeTPP				(S- <i>m</i> -Tol)(HS- <i>m</i> -Tol)FeTPP			
1.989	-0.99246	0.11486	0.04285	1.971	-0.99410	-0.09999	0.04206
2.181	0.11223	0.99191	-0.05924	2.240	0.09978	-0.99498	-0.00702
2.273	-0.04931	-0.05399	-0.99732	2.382	-0.04255	0.00278	-0.99909
(SBzl)(HSBzl)FeTPP				(SPh)(HSPH)FeNH <sub>2</sub> TPP			
1.963	-0.88690	0.46040	0.03797	1.965	-0.93140	0.36116	-0.04535
2.202	0.42949	0.85204	-0.29928	2.242	-0.36399	-0.92409	0.11644
2.265	-0.17014	-0.24912	-0.95341	2.368	-0.00015	-0.12496	-0.99216
(SPh) <sub>2</sub> FeTPP <sup>1-g</sup>				(SPh)(HSPH)FeTPP			
1.962	0.99699	-0.07395	0.02344	1.966	0.94865	-0.31629	0.00518
2.215	-0.07710	-0.97815	0.19306	2.244	0.31631	0.94827	-0.02712
2.336	-0.00865	0.19428	0.98091	2.364	0.00366	0.02737	0.99962

<sup>a</sup> Bond distances for the thiol/thiolate complexes are average distances for the thiol and thiolate ligands. <sup>b</sup> These compounds undergo complex spin equilibria. The anomalously long distance for the *m*-tolyl complex is attributed to an unresolved disorder. <sup>c</sup> An estimate based on the observed<sup>16a</sup> pK<sub>a</sub>'s for 1-propyl and 1-butyl thiols (both 10.65). <sup>d</sup> Reference 16b. <sup>e</sup> These values were obtained from the spectrum of a polycrystalline sample. The principal values obtained from the single-crystal investigation (1.963, 2.202, and 2.265) agree less well with the polycrystalline values than those for the other compounds. This could be a result of the fact that for this compound the X-ray orientation determinations were carried out at room temperature and the ESR measurements were made at 77 K. <sup>f</sup> The estimated experimental uncertainties in  $\Delta$ ,  $V$ , and  $V/\Delta$  are 0.2, 0.1, and 0.03, respectively.  $\Delta$  and  $V$  are given in units of  $\lambda$ , the spin-orbit coupling constant. <sup>g</sup> These  $g$  values are based on a more recent analysis of the data reported previously.<sup>14</sup> <sup>h</sup> In which  $x$  is the vector from the iron atom to the pyrrole nitrogen atom closest to the pseudosymmetry plane of the axial ligand and  $y$  is in the plane of the four pyrrole nitrogen atoms (see Figure 5).

field as measured by  $\Delta$ . The axial ligand field strengths for the series of thiol/thiolate complexes correlate well with the pK<sub>a</sub>'s of the corresponding thiols.<sup>16</sup> It is certainly reasonable that the axial field strength of the bis(benzenethiolate) anion is greater than that of the benzenethiol/benzenethiolate complex.

Blumberg and Peisach<sup>17-21</sup> have demonstrated that plots of rhombicity ( $V/\Delta$ ) vs. tetragonality ( $\Delta$ ) are very useful for the prediction of the nature of the axial ligation in heme proteins. The rhombicity for the series of complexes in Table I is remarkably constant over a relatively wide range of axial field strengths. The rhombicity thus appears to be a very good measure of the asymmetry of the electron distribution on the thiolate sulfur atom and to be independent of the effective charge on that atom. Notice that the rhombicity of the bis(benzenethiolate) anion is virtually identical to that of the thiol/thiolate complexes.

The constancy of the rhombicity extends to other ferric porphyrin complexes with thiolate ligands. Tang et al.<sup>22</sup> have compiled the  $g$  values for more than 30 ferric porphyrin complexes in which one of the axial ligands is a thiolate and the other is a nitrogenous base, a thiol or thioether, or an oxygen donor (DMF or THF). The porphyrins in this series include tetraphenylporphyrin, octaethylporphyrin, and protoporphyrin IX dimethyl

Table II. The Rhombicities of the Low-Spin (Porphinato)iron(III) Thiolate Complexes as a Function of the Sixth Ligand<sup>a</sup>

THF (4)	1.18-1.25	NMeIm (10)	0.97-1.07
THT (5)	1.15-1.18	DMF (4)	0.96-1.05
py (4)	1.03-1.15	primary amine (3)	0.84-0.88
PhSH (2) <sup>b</sup>	1.01-1.03		

<sup>a</sup> These parameters are based on the tabulated  $g$  values of Tang et al.<sup>22</sup> The numbers in parentheses are the number of complexes in each class. <sup>b</sup> The  $g$  values used for FeTPP(SPh)(HSPH) are those in Table I rather than those given by Tang et al.

ester. Analysis of these  $g$  values show that the rhombicity for the entire series falls in the range 0.84-1.25. It is possible, however, within this range to pick out systematic changes that can be attributed to the nature of the sixth ligand (see Table II).

A similar series of 29 complexes with imidazole and imidazolate ligands has been compiled by Quinn, Nappa, and Valentine.<sup>23</sup> This series includes complexes in which one of the axial ligands is an alkoxide or phenoxide. An additional compilation of 11 "highly anisotropic" low-spin complexes with particularly weak nitrogen donors in the axial sites was published by Nigita and Iwaizumi.<sup>24</sup> The rhombicities for this entire group of 40 complexes again fall in a narrow range, 0.47-0.66, but these values are much smaller than those of the thiolate complexes.

The above results can be rationalized empirically by decomposition of the metal-ligand interactions that give rise to the splitting of the  $t_{2g}$  orbitals shown in Figure 1. The interaction between the orbitals and a ligand with a plane of symmetry can be considered to be made up of two parts. The  $\pi$  interaction is that of a ligand with a d orbital antisymmetric with respect to the symmetry plane of the ligand. The  $\pi'$  interaction is that of a ligand with a d orbital symmetric with respect to the symmetry

(16) (a) Patal, Ed. "The Chemistry of the Thiol Group"; Wiley: New York, 1974; Part I, p 398. (b) Danehy, J. P.; Parameswaran, K. N. *J. Chem. Eng. Data* 1968, 13, 386.

(17) Blumberg, W. E.; Peisach, J. "Bioinorganic Chemistry"; Dessy, R., Dillard, J., Taylor, L., Eds.; American Chemical Society: Washington, DC, 1971; *Adv. Chem. Ser. No. 1000* p 271.

(18) Blumberg, W. E.; Peisach, J. "Probes and Structure and Function of Macromolecules and Membranes"; Chance, B., Yonetani, T., Mildvan, A. S., Eds.; Academic Press: New York, 1971 Vol. 2, p 215.

(19) Appleby, C. A.; Blumberg, W. E.; Peisach, J.; Wittenberg, B. A.; Wittenberg, J. B. *J. Biol. Chem.* 1976, 251, 6090.

(20) Brautigam, D. L.; Feinberg, B. A.; Hoffman, B. M.; Margolish, E.; Peisach, J.; Blumberg, W. E. *J. Biol. Chem.* 1977, 252, 574.

(21) Chevion, M.; Peisach, J.; Blumberg, W. E. *J. Biol. Chem.* 1977, 252, 3637.

(22) Tang, S. C.; Koch, S.; Papaefthymiou, G. C.; Foner, S.; Frankel, B. B.; Ibers, J. A.; Holm, R. H. *J. Am. Chem. Soc.* 1976, 98, 2414.

(23) Quinn, R.; Nappa, M.; Valentine, J. S. *J. Am. Chem. Soc.* 1982, 104, 2588.

(24) Migita, C. T.; Iwaizumi, M. *J. Am. Chem. Soc.* 1981, 103, 4378.

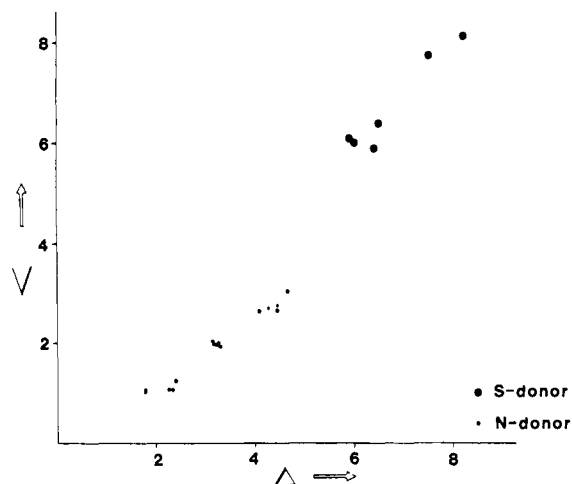


Figure 4.  $V$  vs.  $\Delta$  for Fe<sup>III</sup>TPP thiolate complexes (Table I), Fe<sup>III</sup>TPP imidazole and imidazole complexes,<sup>23</sup> and (protoporphyrin IX)iron(III) pyridine complexes.<sup>24</sup>

plane. In the case of ligands with two planes of symmetry,  $\pi$  and  $\pi'$  are defined with respect to the plane that contains the ligand atoms. With this designation the energies of the three  $t_{2g}$  orbitals can be expressed in terms of the interactions with the pyrrole groups of the porphyrin,  $\pi_p$  and  $\pi'_p$ , and the interactions with the axial ligands,  $\pi_a$  and  $\pi'_a$ . In a complex with the geometry of conformer **1** in Figure 1, the  $d_{xy}$  orbital interacts in a  $\pi'$  fashion with the four pyrrole groups, the  $d_{xz}$  orbital interacts in a  $\pi$  fashion with two of the pyrrole groups and in a  $\pi'$  fashion with the two axial ligands, and the  $d_{yz}$  orbital interacts in a  $\pi$  fashion with two of the pyrrole groups and the two axial ligands. This results in the following expressions for the crystal field parameters

$$V = 2(\pi_a - \pi'_a)$$

$$\Delta = (\pi_a + \pi'_a) + (2\pi_p - 4\pi'_p)$$

Notice that if the axial ligand is similar to the pyrrole group, this model predicts that  $V/\Delta$  should be approximately 2/3. This is consistent with the observation that a wide range of planar nitrogen donors give iron-porphyrin complexes with rhombicities in the range 0.47–0.66.

The intrinsic asymmetry of a ligand, defined as  $(\pi_a - \pi'_a)/(\pi_a + \pi'_a)$ , should to the first approximation be independent of  $\sigma$ -donor strength and distance to the metal atom. To obtain such an asymmetry from the crystal field parameters above requires knowledge of the quantity  $(2\pi_p - 4\pi'_p)$  in the expression for  $\Delta$ . With the assumption that  $\pi_a$  and  $\pi'_a$  scale in the same way as a function of charge on the donor atom and metal-donor distance, one can obtain an estimate of  $(2\pi_p - 4\pi'_p)$  from the  $x$  intercept of a plot of  $V$  vs.  $\Delta$  for a group of similar complexes that differ in  $\sigma$ -donor strength.

Figure 4 shows plots of  $V$  vs.  $\Delta$  for the complexes in Table I, for the FeTPP imidazole and imidazole complexes tabulated by Quinn, Nappa, and Valentine, and for a set of substituted pyridine complexes reported by Nigita and Iwaizumi. These plots indicate that  $(2\pi_p - 4\pi'_p)$  is close to zero. For this reason the rhombicity,  $V/\Delta$ , is a very good measure of the intrinsic asymmetry in complexes where the axial ligands are chemically equivalent and approximately parallel or in cases where the interactions with one of the axial ligands dominate.

If in the thiol/thiolate complexes the interactions of the thiolate ligand dominate, the rhombicity of the benzenethiol/benzenethiolate complex should be the same as that of the bis(benzenethiolate) anion, as is observed. Also supporting the supposition that the rhombicity is dominated by the thiolate ligand is the observation<sup>25</sup> that for ferricytochrome *c*, where one of the axial ligands is a thioether and the other an imidazole, the rhombicity is only 0.58, much lower than that observed for thiolate complexes (vide infra).

In cases where the ligands are of similar strength but differ in intrinsic asymmetry, the observed rhombicity is a composite of the intrinsic asymmetries for the two ligands. For example, in the thiolate complexes with a primary amine as second axial ligand (see Table II), the amine is a relatively strong but very symmetric ligand. The rhombicity of these complexes is probably reduced by a large contribution to  $\Delta$  by the amine ligand. A trans influence produced by the amine ligand could also contribute to the observed reduction.

One can certainly envision symmetric complexes in which the observed rhombicity could be reduced by orthogonal orientations of the axial ligands, but such conformers would be strained and would in any event exhibit some form of Jahn-Teller distortion.

A direct indication of the source of the rhombicity is available from the experimental determination of the  $g$  tensor. On the basis of the above analysis, a carefully selected series of measurements should allow reasonably accurate prediction of the distribution of spin density in a wide range of ferric porphyrin complexes. This report contains the first measurements in such a series.

**Analysis of the  $g$  Tensor Orientations.** Ellipsoid representations of the  $g$  tensors presented in Figure 5 show that the largest  $g$  value in each case occurs with the magnetic field approximately perpendicular to the porphyrin plane. Views down the porphyrin normal are of particular interest in light of the foregoing discussion. A comparison of the six complexes shows that rotation of the pseudosymmetry plane of the axial ligand about the porphyrin normal indeed results in rotation of the principal axes of the  $g$  tensor in the opposite direction.

It appears that the  $g$ -tensor orientation in these complexes is determined almost entirely by the orientation of the thiolate ligand. One of the principal axes of the rhombic field produced by the thiol ligand should approximately bisect the projection of the S-H and S-C bonds in the porphyrin plane. If this interaction was significant, it should be readily apparent in the orientation of the principal axes of the  $g$  tensor. (The proton position is indicated in the drawings of the benzyl and isoamyl complexes.) The absence of a significant contribution from the thiol ligand is consistent with the analysis of the principal  $g$  values in the preceding section.

Views of the  $g$  tensor down the two Fe-N(pyrrole) directions do not reveal any systematic deviation of the longest principal axis from the porphyrin normal. Only the benzylthiol/benzylthiolate complex and the bis(benzenethiolate) anion show significant deviations. As explained in the note to Table I, the benzyl determination is most subject to systematic errors. The 11° deviation in the bis(benzenethiolate) anion is larger than the estimated uncertainty (about 3°), but the uniformity in the results of the other determinations suggests that this deviation results from an error in the measurement.

**Reevaluation of ESR Data for Heme Proteins.** While the investigations described above are, to our knowledge, the first  $g$  tensor determinations for small-molecule iron porphyrin complexes, single-crystal ESR measurements have been made for a number of heme proteins. In addition to the problem of interpretation cited above, the utility of these measurements has been limited by the lack of similar data for small-molecule analogues and by the limited precision with which the structures are known. The situation is also complicated by the fact that in several cases independent determinations of the  $g$  tensor orientation for the same species do not agree. Recent work on the nitrosyl myoglobin complex<sup>26</sup> points up an additional potential problem with the use of room-temperature structural data and low-temperature magnetic resonance data. A summary of the principal  $g$  values and the crystal field parameters for a number of ferric heme proteins is given in Table III.

**Metmyoglobin Azide.** The heme protein for which the largest amount of pertinent data is available is the azide complex of metmyoglobin. There have been three independent ESR deter-

(25) Mailer, C.; Taylor, C. P. S. *Can. J. Biochem.* **1972**, *50*, 1048.

(26) Hori, H.; Ikeda-Saito, M.; Yonetani, T. *J. Biol. Chem.* **1981**, *256*, 7849.

(27) Hori, H. *Biochim. Biophys. Acta* **1971**, *251*, 227.

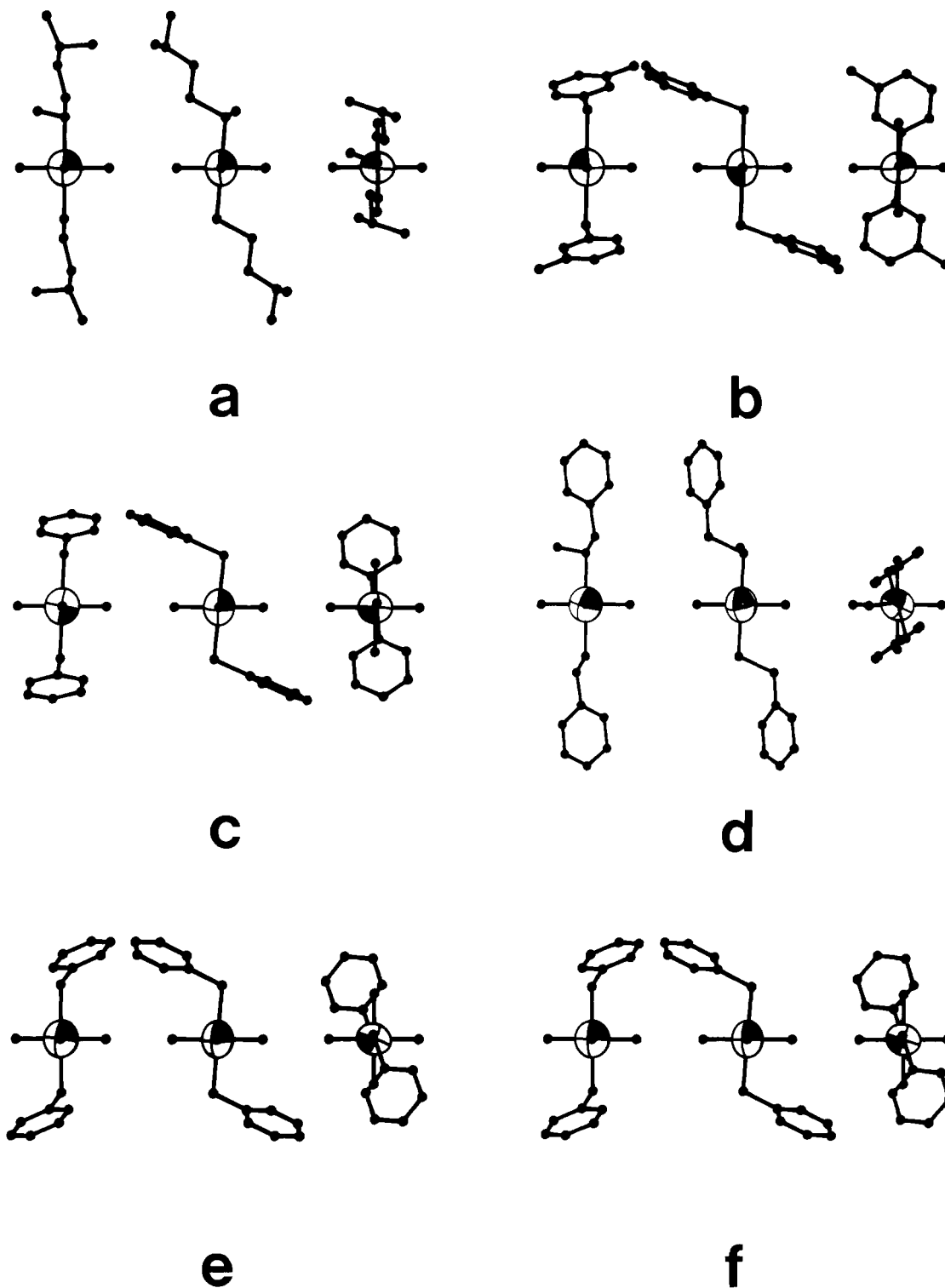


**Figure 5.** The  $g$  tensor representations for the series of complexes in Table I arranged in order of increasing angle between the pseudosymmetry plane of the axial ligand and the iron to pyrrole-nitrogen vector. From left to right the molecular  $x$ ,  $y$ ,  $z$  axes point toward the reader. The complexes are (a) FeTPP(S-3-Me-1-Bu)(HS-3-Me-1-Bu), (b) FeTPP(S-*m*-Tol)(HS-*m*-Tol), (c) FeTPP(SPh) $_2^-$ , (d) FeTPP(SBzl)(HSBzl), (e) FeNH $_2$ TPP-(SPh)(HSPH), and (f) FeTPP(SPh)(HSPH).

minations of the  $g$  tensor orientation, and the orientation of the electric field gradient tensor has been determined from single-crystal Mössbauer measurements. The original  $g$  tensor determination by Gibson and Ingram<sup>28</sup> was completed before the structure of myoglobin was known. In 1964 Stryer, Kendrew,

(28) Gibson, J. F.; Ingram, J. F. *Nature (London)* **1957**, *180*, 29.

(29) Schleyer, H. *Ann. N. Y. Acad. Sci.* **1973**, *212*, 57.

(30) Tsai, R.; Yu, C. A.; Gunsalus I. C.; Pelsach, J.; Blumberg, W. H.; Orme-Johnson, W. H.; Beinert, H. *Proc. Natl. Acad. Sci. U.S.A.* **1970**, *66*, 1157.

**Table III.** The  $g$  Values and Crystal Field Parameters for a Selection of Heme Proteins<sup>a</sup>

	$g_x$	$g_y$	$g_z$	$\Delta$	$V$	$V/\Delta$	ref
Mb-CN	0.93	1.89	3.45	3.3	0.92	0.28	27
Mb-N $_3$	1.72	2.22	2.80	4.7	2.4	0.51	28
Mb-imi	1.53	2.26	2.91	3.3	1.9	0.58	27
cyt $b_5$	1.47	2.26	2.95	3.1	1.8	0.58	29
cyt $c$	1.25	2.25	3.06	2.6	1.5	0.58	25
P450	1.91	2.26	2.45	5.1	4.6	0.90	30

<sup>a</sup> Mb = metmyoglobin, imi = imidazole, and cyt = cytochrome.

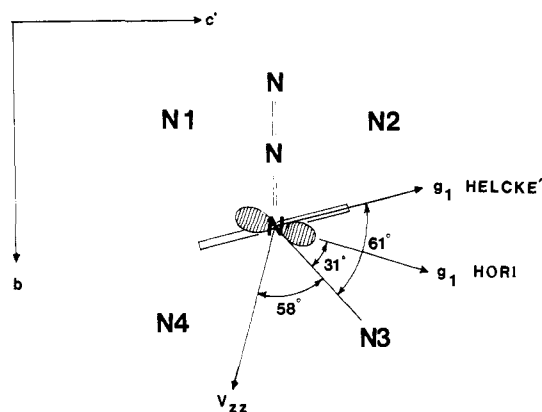


**Figure 6.** The orientations of the principal axes of the  $g$  tensor and EFG tensor in the azide complex of metmyoglobin. The directions of the smallest  $g$  values as measured by Helcké et al. and Hori are indicated.

and Watson<sup>9</sup> reported the structure of the azide complex of metmyoglobin. They found that the linear azide ion makes an angle of  $21^\circ$  with the heme plane and that the projection on the heme plane points toward one of the methine bridge carbon atoms. In 1967 an independent  $g$  tensor determination by Helcké, Ingram, and Slade<sup>8</sup> was found to agree well with that of Gibson and Ingram. With the availability of structural data, these investigators found that the largest principal axis of the  $g$  tensor is close to the heme normal and that the principal axis corresponding to the smallest  $g$  value was parallel to the plane of the coordinated imidazole ring. They took this to mean that the imidazole orientation governed the orientation of the  $g$  tensor. Several investigators have questioned this assignment, however, on the basis of the magnitude of the splitting between the " $d_{xz}$ " and " $d_{yz}$ " levels as derived from the principal  $g$  values. Kotani<sup>2</sup> (1964) estimated the rhombic field produced by the imidazole to be on the order of  $60\text{ cm}^{-1}$ , much smaller than the derived splitting ( $\sim 1000\text{ cm}^{-1}$ ). On this basis he attributed the anisotropy in the heme plane mainly to the asymmetric position of the azide ion. Mizuhashi<sup>31</sup> (1969) estimated the rhombic field produced by a covalent azide to be on the order of  $100\text{ cm}^{-1}$  and showed that the combination of dynamic Jahn-Teller distortion and the small rhombic fields produced by the ligands could account for the large observed anisotropy. Neither of these investigations, however, addressed the question of the orientation of the  $g$  tensor.

In a 1971 determination, Hori<sup>27</sup> found again that the largest  $g$  value was close to the heme normal, but in this determination the orientation of the principal axes in the heme plane differed by about  $30^\circ$  from that obtained previously. This determination appears to differ from the others in the sign of  $g_{bc}$ .

Recently two groups have studied the Mössbauer spectrum of Mb-azide. Rhynard, Lang, Spartialian, and Yonetani<sup>32a</sup> demonstrated that it is possible to obtain the relative orientation of the cubic axes of the ligand field and the principal axes of the  $g$  tensor from Mössbauer spectra of polycrystalline samples. Harami<sup>32b</sup> has reported a single-crystal Mössbauer investigation in which he determined the orientation of the electric field gradient (EFG) tensor. In this investigation Harami used the analysis of Oosterhuis and Lang<sup>11</sup> to relate the orientation of the EFG and  $g$  principal axis systems. He showed that the EFG measurements were consistent with the  $g$  tensor determination of Helcké et al. but not with that of Hori. In the absence of molecular orbital calculations for the Mb-azide complex, Harami deferred attributing the asymmetry in the heme plane to any of the various sources that have been suggested.

The ESR results of Helcké, Ingram, and Slade, when interpreted by the approach of Oosterhuis and Lang, and the Mössbauer results of Harami are consistent with the estimates

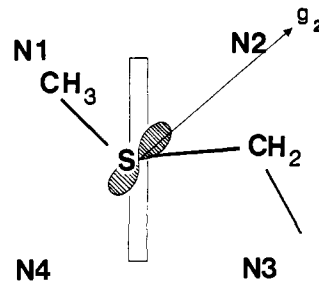


**Figure 7.** The orientation of the principal axes of the  $g$  tensor and partially filled orbital in horse cytochrome  $c$ . The bar indicates the orientation of the coordinated imidazole. The numbering system is that used by Mailer and Taylor.<sup>25</sup>

by Kotani and Mizuhashi of the relative rhombic fields produced by the imidazole and azide ligands. Both of the experimental investigations (but not that of Hori) indicate partial occupation of the orbital indicated in Figure 6. The numerically largest value of the EFG ( $V_{zz}$ ) should, to the first approximation, be normal to the plane of the partially occupied orbital. In the heme plane, reflection of  $g_2$  across an Fe-N vector should place it in the plane defined by the partially occupied orbital.

The proposed orientation is consistent with the azide ion being a stronger  $\pi$  donor than the imidazole of the coordinated histidine. The rotation of  $V_{zz}$  from the projection of the azide in the heme plane is in the direction expected for a contribution of the imidazole to the rhombic field. Taken at face value, the experimental results indicate that the azide ion is a stronger, but not much stronger,  $\pi$  donor than imidazole. It is not clear, however, that the difference in the direction between the azide projection and  $V_{zz}$  is significant.

**Ferricytochrome  $c$ .** On the basis of NMR measurements Redfield and Gupta<sup>33</sup> described the distribution of spin density in the ferric form of horse heart cytochrome  $c$ . In the following year, Mailer and Taylor<sup>25</sup> determined the  $g$  tensor orientation from single-crystal ESR measurements. The results of these two determinations appear to be consistent, although in a later publication Taylor<sup>5</sup> stated that there was an alternative interpretation of his data that differed considerably from the original report. This alternative interpretation is inconsistent with the results of Redfield and Gupta. In a more recent NMR investigation, Keller and Wuthrich<sup>34</sup> also found that their results were consistent with the original assignment by Mailer and Taylor.

Figure 7 shows the orientation of  $g_2$  from the original report of Mailer and Taylor, the orientation of the partially filled orbital based on an analysis following Oosterhuis and Lang,<sup>11</sup> and the orientations of the coordinated imidazole and thioether groups from a recent high-resolution structure determination by Takano and Dickerson.<sup>35</sup> These results indicate that the thioether ligand strongly influences the orientation of the partially filled orbital. This is consistent with NMR observations by Seen, Keller, and Wuthrich.<sup>36</sup> These investigators pointed out that in ferricytochrome  $c$ -551, while the overall structure around the heme is very similar to that of ferricytochrome  $c$ , the methyl group of the coordinated methionine takes up the alternate position close to N4 rather than N1 and that on the basis of the shifts of the thioether methyl resonances of the heme, the  $g$  tensor orientation in this protein differs from that in horse ferricytochrome  $c$  by a rotation of approximately  $90^\circ$  about the heme normal.

**Metmyoglobin Cyanide.** The situation with the cyanide complex of metmyoglobin is more complicated than that of the two previous materials. First is the fact that the rhombicity of this complex, 0.28, is anomalously low. The low rhombicity does not result just from a large contribution of the cyanide ligand to the  $\Delta$ ; the  $V$

(33) Redfield, A. G.; Gupta, R. K. *Cold Spring Harbor Symp. Quant. Biol.* **1971**, *36*, 405. In this report the relationship between the spin density distribution and the  $g$  tensor orientation is misstated.

(34) Keller, R. M.; Wuthrich, K. *Biochim. Biophys. Acta* **1978**, *533*, 195.

(35) Takano, T.; Dickerson, R. E. *J. Mol. Biol.* **1981**, *153*, 95.

(36) Seen, H.; Keller, R. M.; Wuthrich, K. *Biochem. Biophys. Res. Commun.* **1980**, *92*, 1362. Keller, R. M.; Wuthrich, K. *Ibid.* **1978**, *83*, 1132.

(31) Mizuhashi, S. *J. Phys. Soc. Jpn.* **1969**, *26*, 468.

(32) (a) Rhynard, D.; Lang, G.; Spartialian, K.; Yonetani, T. *J. Chem. Phys.* **1979**, *71*, 3715. (b) Harami, T. *J. Chem. Phys.* **1979**, *71*, 1309.

is also much lower than other hemes with an imidazole ligand. This small  $V$  could result from opposing contributions of the two axial ligands or more likely from a decrease in the Fe-imidazole interaction caused by the large trans influence of the cyanide ligand.

The orientation of the  $g$  tensor has been determined from ESR measurements by Peisach, Blumberg, and Wyluda<sup>37</sup> and by Hori,<sup>26</sup> and from NMR measurements by Shulman, Glarum, and Karplus.<sup>38</sup> The measurements by Peisach et al. appear to be consistent with the NMR measurements but differ drastically from those of Hori. Peisach et al. find that in the cyanide complex the largest  $g$  value in the heme plane corresponds to the projection of the imidazole ring on the heme plane (while for the azide complex Helcké et al. found that the smallest  $g$  value corresponds to the projection of the imidazole ring). Hori, on the other hand, found that the  $g$  tensor orientations of the azide, cyanide, and imidazole complexes of myoglobin are very similar.

Further analysis of the magnetic resonance data will require additional consideration of both the protein structural data and magnetic resonance data for small-molecule cyanide complexes. Although X-ray data for the complex are available,<sup>39</sup> we do not as yet have specific information on the orientation of the cyanide ligand. Preliminary results in this laboratory indicate that the cyanide ligand, unlike any of the other ligands discussed above, functions as a  $\pi$  acceptor. Complete  $g$  tensor determinations of several (porphinato)iron(III) cyanide complexes now in progress

(37) Peisach, J.; Blumberg, W. E.; Wyluda, B. J. *Eur. Biophys. Congr. Proc.*, 1st 1971, 1, 109.

(38) Shulman, R. G.; Glarum, S. H.; Karplus, M. *J. Mol. Biol.* 1971, 57, 93.

(39) Deatherage, J. F.; Loe, R. S.; Andersen, C. M.; Moffat, K. J. *Mol. Biol.* 1976, 104, 687. In this paper the authors refer to: Bretscher P. A., Ph.D. Thesis, University of Cambridge, 1968.

should provide additional insight.

## Conclusions

Electron spin resonance  $g$  tensor determinations for a series of low-spin (tetraphenylporphinato)iron(III) thiolate complexes demonstrate that while the relationship between axial ligand orientation and the orientation of the principal axes of the  $g$  tensor is not intuitively obvious, it is in complete accord with a simple model of metal-ligand bonding. Crystal field analysis of the principal  $g$  values for the series of complexes gives an excellent correlation between the tetragonality of the complex ( $\Delta$ ) and the  $pK_a$  of the corresponding thiol. The rhombicity ( $V/\Delta$ ) is found to be essentially constant over a wide range of acid strengths.

The bright prospect that single-crystal ESR measurements could provide a detailed picture of the electronic structure of heme proteins has to some extent fallen under a shadow cast by a collection of confusing and apparently inconsistent results. The present investigation suggests, however, that with proper interpretation based on control experiments with well-characterized small-molecule analogues, a wealth of information is indeed available from such measurements.

**Acknowledgment.** This work was supported by a grant from the National Science Foundation (No. CHE 81-10285) and by the donors of the Petroleum Research Fund, administered by the American Chemical Society.

**Registry No.** (S-3-Me-1-Bu)(HS-3-Me-1-Bu)FeTPP, 85565-22-6; (SBzl)(HSBzl)FeTPP, 85565-23-7; (SPh)<sub>2</sub>FeTPP<sup>-</sup>, 77321-78-9; (S-*m*-Tol)(HS-*m*-Tol)FeTPP, 85565-24-8; (SPh)(HSPh)FeNH<sub>2</sub>TPP, 85565-25-9; (SPh)(HSPh)FeTPP, 54959-14-7; ferricytochrome *c*, 9007-43-6.

**Supplementary Material Available:** A table of the X-ray and ESR data used to generate Figure 5 (6 pages). Ordering information is given on any current masthead page.

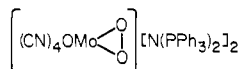
## <sup>17</sup>O NMR as a Tool for Studying Oxygenated Transition-Metal Derivatives: First Direct <sup>17</sup>O NMR Observations of Transition-Metal-Bonded Peroxidic Oxygen Atoms. Evidence for the Absence of Oxo-Peroxo Oxygen Exchange in Molybdenum(VI) Compounds

Michèle Postel,<sup>\*1a</sup> Christian Brevard,<sup>1b</sup> Henri Arzoumanian,<sup>1c</sup> and Jean G. Riess<sup>1a</sup>

Contribution from the Laboratoire de Chimie Minérale Moléculaire, Equipe de Recherche Associée au CNRS, 06034 Nice, France, Bruker-Spectrospin, 67160 Wissembourg, France, and I.P.S.O.I., Faculté des Sciences de St Jérôme, 13397 Marseille-Cedex 4, France.

Received November 12, 1982

**Abstract:** The first high-resolution <sup>17</sup>O NMR observations of peroxidic oxygen atoms bonded to transition metals are reported for <sup>17</sup>O-enriched



as well as for nonenriched alkylperoxo derivatives of platinum. The chemical shifts of the oxo group in a series of Mo(VI) derivatives are also reported. The results are interpreted to evaluate the practicability of <sup>17</sup>O NMR as a tool to investigate the oxygen chemistry of the transition elements. In the case of the oxo-peroxo Mo(VI) derivative, direct <sup>17</sup>O NMR evidence is given that the oxo and peroxo groups do not exchange.

There exist a wide range of molecular transition-metal compounds containing oxygen atoms in their coordination sphere,<sup>2</sup>

many of which are presently receiving considerable attention for their interest as reagents, catalysts, or key intermediates in selective